J|A|C|S
ARTICLES

Mechanistic Studies of Platinum(II)-Catalyzed Ethylene Dimerization: Determination of Barriers to Migratory Insertion in Diimine Pt(II) Hydrido Ethylene and Ethyl Ethylene Intermediates

Masashi Shiotsuki, Peter S. White, Maurice Brookhart,* and Joseph L. Templeton*

Contribution from the Department of Chemistry, University of North Carolina at Chapel Hill, Chapel Hill, North Carolina 27599-3290

Received November 22, 2006; E-mail: mbrookhart@unc.edu

Abstract: The diimine platinum(II) ethylene hydride complex [(N^N)Pt(H)(ethylene)][BAr′$_4$] (**1**, N^N = [(2,6-$Me_2C_6H_3$)N=C(An)−C(An)=N(2,6-$Me_2C_6H_3$)], An = 1,8-naphthalenediyl, Ar′ = 3,5-$(CF_3)_2C_6H_3$) was prepared by protonation of the diethyl complex (N^N)$PtEt_2$ with [$H(OEt_2)_2$][BAr′$_4$]. The energy barrier to interchange of the platinum hydride with the olefinic hydrogens in **1** was determined to be 19.2 kcal/mol by spin saturation transfer experiments. Complex **1** initiates ethylene dimerization; the ethyl ethylene complex (N^N)Pt(Et)(ethylene)$^+$ (**2**) has been identified as the catalyst resting state. Trapping of **1** by ethylene to yield **2** is a second-order process; kinetic studies suggest this occurs via trapping of a reversibly formed β-agostic ethyl complex. Complex **2** has been isolated and characterized by X-ray crystallography. The barrier to migratory insertion of **2**, the turnover-limiting step in catalysis, was determined to be 29.8 kcal/mol. The 1-butene hydride complex, (N^N)Pt(H)(1-butene)$^+$ (**3**), is a key intermediate in the dimerization cycle and has also been isolated and characterized. Surprisingly rapid rates of degenerate associative exchange of free ethylene with bound ethylene in complexes **1** and **2** as well as the rate of degenerate exchange of free nitrile with bound nitrile in (N^N)Pt(Et)(CH_3CN)$^+$ are reported.

Introduction

Investigations of late transition metal-catalyzed olefin polymerizations, oligomerizations, and dimerizations have attracted attention from a large number of academic and industrial research groups.[1−9] Our group first reported that cationic aryl-substituted α-diimine complexes of Ni(II) and Pd(II) bearing ortho substituents on the aryl rings were active catalysts for homopolymerization and oligomerization of ethylene and α-olefins. Incorporating ortho-aryl substituents proved to be a critical design feature that led to reduction of the rate of chain transfer and thus production of high molecular weight polymers. Working with the Versipol group at DuPont, these investigations were expanded to include a broad range of monomers and catalysts incorporating numerous α-diimine ligands.[10−13] Variable temperature NMR spectroscopic studies established that the cationic metal alkyl complexes, (diimine)M−R$^+$ (M = Ni, Pd; R = alkyl groups C_nH_{2n+1}, $n > 1$) adopt β-agostic structures and provided information concerning the energetics of metal migration along the alkyl chains in such complexes.[12,14−18] The barriers to migratory insertion in (diimine)M(ethylene)R$^+$ complexes, frequently the catalyst resting state during ethylene polymerization, were found to be in the range 13−14 kcal/mol for Ni(II) complexes and ca. 5 kcal/mol higher for Pd(II) complexes, 17−19 kcal/mol.

Little is known concerning the structure, dynamics, and catalytic chemistry of the corresponding Pt(II) diimine complexes. Ruffo[19] has reported the synthesis of the cationic methyl

---

(1) Ittel, S. D.; Johnson, L. K.; Brookhart, M. *Chem. Rev.* **2000**, *100*, 1169−1203.
(2) Mecking, S. *Coord. Chem. Rev.* **2000**, *203*, 325−351.
(3) Gibson, V. C.; Spitzmesser, S. K. *Chem. Rev.* **2003**, *103*, 283−315.
(4) Fischer, K.; Jonas, K.; Misbach, P.; Stabba, R.; Wilke, G. *Angew. Chem., Int. Ed. Eng.* **1973**, *12*, 943−953.
(5) Cornils, B.; Herrmann, W. A. *Applied Homogeneous Catalysis with Organometallic Compounds*; VCH Verlagsgesellshaft mbH: Weinheim, 1996.
(6) Parshall, G. W.; Ittel, S. D. *Homogeneous Catalysis*, 2nd ed.; John Wily & Sons: New York, 1992; p 72.
(7) Pillai, S. M.; Ravindranathan, M.; Sivaram, S. *Chem. Rev.* **1986**, *86*, 353−399.
(8) Speiser, F.; Braunstein, P.; Saussine, L. *Acc. Chem. Res.* **2005**, *38*, 784−793.
(9) Britovsek, G. J. P.; Bruce, M.; Gibson, V. C.; Kimberley, B. S.; Maddox, P. J.; Mastroianni, S.; McTavish, S. J.; Redshaw, C.; Solan, G. A.; Strömberg, S.; White, A. J. P.; Williams, D. J. *J. Am. Chem. Soc.* **1999**, *121*, 8728−8740.
(10) Leatherman, M. D.; Svejda, S. A.; Johnson, L. K.; Brookhart, M. *J. Am. Chem. Soc.* **2003**, *125*, 3068−3081.
(11) Gates, D. P.; Svejda, S. A.; Oñate, E.; Killian, C. M.; Johnson, L. K.; White, P. S.; Brookhart, M. *Macromolecules* **2000**, *33*, 2320−2334.
(12) Tempel, D. J.; Johnson, L. K.; Huff, R. L.; White, P. S.; Brookhart, M. *J. Am. Chem. Soc.* **2000**, *122*, 6686−6700.
(13) Brookhart, M. S.; Johnson, L. K.; Killian, C. M.; Arthur, S. D.; Feldman, J.; McCord, E. F.; McLain, S. J.; Kreutzer, K. A.; Bennett, M. A.; Coughlin, E. B.; Ittel, S. D.; Parthasarathy, A.; Tempel, D. J. E. I. Du Pont de Nemours & Co. and University of North Carolina at Chapel Hill. Patent PCT WO9623010, April 3, 1995.
(14) Killian, C. M.; Johnson, L. K.; Brookhart, M. *Organometallics* **1997**, *16*, 2005−2007.
(15) Svejda, S. A.; Johnson, L. K.; Brookhart, M. *J. Am. Chem. Soc.* **1999**, *121*, 10634−10635.
(16) Rix, F. C.; Brookhart, M. *J. Am. Chem. Soc.* **1995**, *117*, 1137−1138.
(17) Johnson, L. K.; Killian, C. M.; Brookhart, M. *J. Am. Chem. Soc.* **1995**, *117*, 6414−6415.
(18) Malinoski, J. M.; Brookhart, M. *Organometallics* **2003**, *22*, 5324−5335.
(19) Fusto, M.; Giordano, F.; Orabona, I.; Ruffo, F. *Organometallics* **1997**, *16*, 5981−5987.

10.1021/ja068118o CCC: $37.00 © 2007 American Chemical Society

Scheme 1. Pt(II) Aryl-Substituted Diimine Complexes **1**−**3**

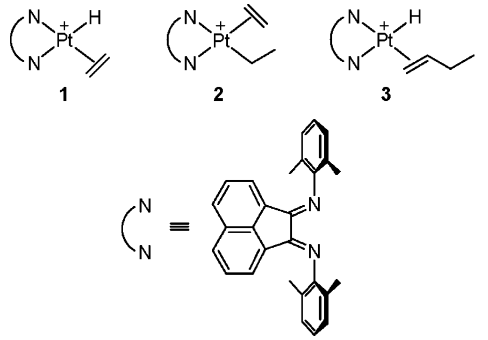

Scheme 2. Synthesis of Ethylene Hydride Complex **1**

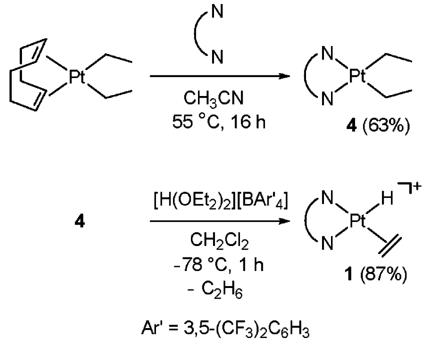

olefin complexes $[ArN{=}C(Me){-}C(Me)C{=}NAr]Pt(CH_3)(olefin)^+$ (Ar = 2,6-*i*-$Pr_2C_6H_3$, olefin = ethylene, propylene, styrene; Ar = 2,6-$Et_2C_6H_3$, olefin = ethylene). Line-broadening of the bound ethylene resonance was observed in the presence of free ethylene but no quantitative exchange rates were reported. An X-ray diffraction study of a single crystal of the methyl ethylene complex for Ar = 2,6-$Et_2C_6H_3$ showed, as expected, that the C−C axis of the ethylene ligand and the aryl rings lie nearly perpendicular to the coordination square plane. No insertion chemistry of these simple olefin complexes was noted although a later report by Ruffo[20] showed that migratory insertion occurs at 60 °C in the electron deficient olefin complex $[ArN{=}C(Me){-}C(Me)C{=}NAr]Pt(CH_3)(methyl\ acrylate)^+$ (Ar = 2,6-$Et_2C_6H_3$) to yield a chelate complex involving the ester carbonyl functionality analogous to that observed in the Pd(II) congener. DFT calculations suggest that the aryl-substituted (diimine)Pt-(H)(ethylene)$^+$ complex should be a classical hydride and that the barrier to alkyl migration in the analogous alkyl ethylene complex should be ca. 26 kcal/mol, much higher than the Ni-(II) (10−11 kcal/mol) and Pd(II) (16−18 kcal/mol) barriers.[21−23]

There are several additional reports relevant to the work described here. Numerous square planar platinum(II) hydrido olefin complexes bearing bidentate ligands have been characterized. Complexes bearing bidentate nitrogen ligands include (κ^2-trispyrazolylborate)Pt(H)(olefin)$^+$ [24] and (β-diiminate)Pt(H)-(olefin)[25,26] systems. In each of these classes of complexes, the olefin hydrides adopt classical hydride structures rather than β−agostic geometries. Spencer has reported cationic platinum-(II) olefin hydrides supported by a series of bidentate phosphines.[27−30] The structures of these species can be classical olefin hydrides or β-agostic alkyl complexes depending on the P−Pt−P angle, the bulk of the substituents on phosphorus, and the substituents on the olefin. The energy difference between the agostic and terminal hydride structures in these complexes is small. The sole report of catalytic ethylene dimerization by a homogeneous Pt(II) complex is that by Roddick who observed that $[(C_2F_5)_2PCH_2CH_2P(C_2F_5)_2]Pt(CH_3)(OTf)$ initiates dimerization at 65 °C in methylene chloride. A coordination-insertion mechanism was established but neither the intermediate hydride nor the ethyl ethylene complex could be observed.[31] Vitagliano has reported Pt(II)-catalyzed codimerization of ethylene and substituted olefins but a coordination-insertion mechanism does not apply. Rather the C−C bond forms by direct attack of the nucleophilic substituted olefin on the electrophilic Pt(II)-bound ethylene.[32,33]

We report here the synthesis, characterization and chemistry of the Pt(II) aryl-substituted diimine complexes **1**, **2**, and **3** (Scheme 1). Complex **1**, the ethylene hydride complex, initiates catalytic ethylene dimerization, whereas complex **2**, the ethyl ethylene complex, is the catalyst resting state, and complex **3**, the butene hydride, is a key intermediate in the catalytic cycle. Migratory insertion barriers are reported for **1** and **2** along with the kinetics and mechanism for conversion of **1** to **2**, which permits quantitative comparison to the Ni(II) and Pd(II) analogues.

Results and Discussion

Synthesis of (Diimine)PtEt$_2$ (4). α-Diimine diethyl platinum complex **4** was synthesized by treatment of (cod)PtEt$_2$ (cod = 1,5-cyclooctadiene) with excess α-diimine ligand, N^N (N^N = $[(2,6\text{-}Me_2C_6H_3)N{=}C(An){-}C(An){=}N(2,6\text{-}Me_2C_6H_3)]$, An = 1,8-naphthalenediyl), in acetonitrile solution (Scheme 2). After heating at 55 °C for 16 h, the solvent was removed in vacuo and (N^N)PtEt$_2$ (**4**) was purified by column chromatography on alumina. Recrystallization from CH_2Cl_2/pentane provided **4** as green microcrystals. Complex **4** is air stable in the solid state and is moderately stable in solution (ca. 1 day). The diethyl palladium analogue[34] has been prepared by the reaction of (N^N)PdCl$_2$ with 2 equiv of EtMgCl, but the same method was not successful for preparing the (diimine)Pt diethyl complex.[35,36]

---

[20] Ganis, P.; Orabona, I.; Ruffo, F.; Vitagliano, A. *Organometallics* **1998**, *17*, 2646−2650.

[21] Strömberg, S.; Zetterberg, K.; Siegbahn, P. E. M. *J. Chem. Soc., Dalton Trans.* **1997**, 4147−4152.

[22] Musaev, D. G.; Froese, R. D. J.; Morokuma, K. *New. J. Chem.* **1997**, *21*, 1269−1282.

[23] Musaev, D. G.; Morokuma, K. *Top. Catal.* **1999**, *7*, 107−123.

[24] Reinartz, S.; Baik, M.-H.; White, P. S.; Brookhart, M.; Templeton, J. L. *Inorg. Chem.* **2001**, *40*, 4726−4732.

[25] Fekl, U.; Goldberg, K. I. *J. Am. Chem. Soc.* **2002**, *124*, 6804−6805.

[26] Fekl, U.; Kaminsky, W.; Goldberg, K.; I. *J. Am. Chem. Soc.* **2003**, *125*, 15286−15287.

[27] Mole, L.; Spencer, J. L.; Carr, N.; Orpen, A. G. *Organometallics* **1991**, *10*, 49−52.

[28] Carr, N.; Dunne, B. J.; Mole, L.; Orpen, A. G.; Spencer, J. L. *J. Chem. Soc., Dalton Trans.* **1991**, 863−871.

[29] Carr, N.; Mole, L.; Orpen, A. G.; Spencer, J. L. *J. Chem. Soc., Dalton Trans.* **1992**, 2653−2662.

[30] Spencer, J. L.; Mhinzi, G. S. *J. Chem. Soc., Dalton Trans.* **1995**, 3819−3824.

[31] White, S.; Bennett, B. L.; Roddick, D. M. *Organometallics* **1999**, *18*, 2536−2542.

[32] Hahn, C.; Cucciolito, M. E.; Vitagliano, A. *J. Am. Chem. Soc.* **2002**, *124*, 9038−9039.

[33] Cucciolito, M. E.; D'Amora, A.; Vitagliano, A. *Organometallics* **2005**, *24*, 3359−3361.

[34] Shultz, L. H.; Brookhart, M. *Organometallics* **2001**, *20*, 3975−3982.

[35] (Diimine)PtCl$_2$ was prepared by modified procedure according to the following paper: van Asselt, R.; Elsevier, C. J.; Amatore, C.; Jutand, A. *Organometallics* **1997**, *16*, 317−328.

[36] Here, the following analogous α-diimine ligand was used: $[(2,4,6\text{-}Me_3C_6H_2)N{=}C(An){-}C(An){=}N(2,4,6\text{-}Me_3C_6H_2)]$. The main product was confirmed as mono alkylated (diimine)Pt complex by ^1H NMR spectrum.

Complex **4** was fully characterized by ^{1}H and ^{13}C NMR spectroscopy. The pattern of the aromatic signals of the diimine ligand and the appearance of one singlet for the four xylyl methyl substituents reveals the presence of two mirror planes, consistent with C_{2v} symmetry for **4**. The methyl and methylene hydrogens of the ethyl ligands appear as a triplet at 0.73 ppm ($^3J_{\text{Pt-C}} = 85$ Hz) and a quartet at 2.05 ppm ($^2J_{\text{Pt-H}} = 95$ Hz), respectively. As in the ^{1}H NMR spectrum, the aromatic region of the ^{13}C NMR spectrum confirms the symmetry of **4** (see Experimental Section). The xylyl methyl groups of the diimine ligand appear at 17.5 ppm whereas the methyl and methylene carbons of the ethyl ligands are found at 17.8 and −0.3 ppm ($^1J_{\text{Pt-H}} = 886$ Hz), respectively.

Whereas there is ample precedent in the literature for dialkyl platinum complexes bearing a bidentate nitrogen ligand, there are few examples of diethyl analogues.[37,38] One relevant example is (2,2′-bipyridyl)PtEt$_2$ reported by Chaudhury et al.;[38] reactivity studies of (2,2′-bipyridyl)PtEt$_2$ were limited by low solubility in organic solvents and a satisfactory NMR spectrum was not reported.

Synthesis and Reactivity of the Platinum Ethylene Hydride Complex, [(N^N)Pt(H)(ethylene)][BAr′$_4$] (1). Diethyl platinum complex **4** was converted to the cationic ethylene hydride complex, [(N^N)Pt(H)(ethylene)][BAr′$_4$] (**1**), by protonation with a slight excess of [H(OEt$_2$)$_2$][BAr′$_4$] (Ar′ = 3,5-(CF$_3$)$_2$C$_6$H$_3$) in diethyl ether at −78 °C (Scheme 2). Complex **1** was isolated as an air stable, light orange powder by repeated recrystallization from CH$_2$Cl$_2$/pentane. In the ^{1}H NMR spectrum of **1** in CD$_2$Cl$_2$, the coordinated ethylene exhibited a broad singlet at 4.02 ppm with platinum satellites ($^2J_{\text{Pt-H}} = 64$ Hz), and the hydride resonance appeared as a sharp singlet at −21.7 ppm with coupling to platinum of 1107 Hz. The four methyl groups of the xylyl substituents display two singlets at 2.31 and 2.42 ppm, consistent with different ligands trans to the two nitrogen donors.

To the best of our knowledge, there is only one earlier example of a cationic platinum hydride ethylene complex bearing a bidentate N-donor ligand, namely [κ^2-(HPz*)BH-(Pz*)$_2$]Pt(H)(ethylene)$^+$ (Pz* = 3,5-dimethylpyrazolyl).[24] Consistent with data for **1**, the hydride resonance in the protonated pyrazolylborate case appears at −22.19 ppm with coupling to platinum of 1048 Hz and the coordinated ethylene signals appear at 3.86 and 3.51 ppm. Other reported olefin-coordinated analogues bearing bidentate N donor ligands[25,26,39−46] have chemical shifts for the hydride between −17 and −30 ppm and Pt−H coupling constants from 1045 to 1360 Hz.

Cationic platinum hydride olefin complexes bearing bidentate phosphine ligands show different characteristics in their ^{1}H NMR spectra.[27−30] Because of rapid interchange between a hydride olefin structure and a β-agostic alkyl structure on the NMR time scale, distinct hydride signals can be observed only by low temperature ^{1}H NMR. These phosphine complexes have hydride resonances in the range of −1.0 to −5.0 ppm, far downfield from the hydride resonance of **1**, with a small to medium coupling constant to platinum (70∼700 Hz) due to decreased Pt−H interactions. A reported β-agostic ethyl Pd analogue bearing an α-diimine ligand shows a broad triplet ($^2J_{\text{H-H}} = 16$ Hz) at −8.90 ppm at −130 °C in CDCl$_2$F, corresponding to a β-agostic hydrogen resonance.[34]

When the ethylene hydride complex **1** in methylene chloride is sparged with ethylene at room temperature the ethyl ethylene complex, [(N^N)Pt(Et)(ethylene)][BAr′$_4$] (**2**), is formed via hydride migration and trapping by ethylene. Complex **2** was isolated in high yields as an air stable orange powder. The analogous acetonitrile-trapped ethyl Pt complex, [(N^N)Pt(Et)-(CH$_3$CN)][BAr′$_4$] (**5**), was also formed *in situ* and observed via NMR spectroscopy.

(1)

1

2: L = ethylene (88%)
5: CH$_3$CN (in situ)

In the ^{1}H NMR spectrum of **2**, the hydrogens of the coordinated ethylene resonate slightly upfield of the analogous signal in **1**, appearing as a broad singlet at 3.96 ppm with platinum satellites ($^2J_{\text{Pt-H}} = 72$ Hz). A triplet at 0.39 ppm and a quartet at 0.99 ppm ($^2J_{\text{Pt-H}} = 74$ Hz) are observed, consistent with formation of a Pt-ethyl group. All protons of the naphthyl moiety exhibit different shifts, and two xylyl methyl signals appear as singlets at 2.28 (6H) and 2.37 (6H) ppm consistent with only mirror symmetry for **2**. The ^{1}H NMR spectrum of the nitrile-trapped analogue, **5**, looks quite similar to that for **2** but contains a broad singlet at 2.03 ppm attributable to coordinated nitrile and lacks the four proton ethylene signal.

The structure of complex **2** was confirmed by X-ray analysis. Crystallographic data and an ORTEP drawing are shown in Table 1 and Figure 1, respectively. The expected square planar geometry of **2** is clearly evident. The sum of the four cis L−Pt−L′ angles around the Pt center is 360.07°, and the distance between the platinum atom and the least-squares mean plane based on C3, N5, N26, and the centroid of C1−C2 bond is 0.014 Å. The bond length of Pt−N26 (2.181(5) Å) is longer than that of the Pt−N5 bond (2.065(5) Å) by more than 0.1 Å; these distances are in the range of reported examples of (diimine)Pt(R)(olefin)$^+$ complexes.[19,47] The strong σ donation of the ethyl group results in the elongation of the trans Pt1−N26 bond. The same tendency has been reported for a methyl analogue, (diimine)Pt(CH$_3$)(ethylene)$^+$.[19]

Ethylene Dimerization. Under excess ethylene, complex **2** catalyzes ethylene dimerization to produce 1-butene together with *cis*- and *trans*-2-butene (eq 2). The reaction was monitored by ^{1}H NMR spectroscopy using a 1,1,2,2-tetrachloroethane-d_2 (CDCl$_2$CDCl$_2$) solution of catalyst **2** and 30−60 equiv of ethylene. The dimerization reaction at 100 °C is very clean; 1-butene and *cis*- and *trans*-2-butenes are the only products

---

(37) Uchida, H.; Sai, A.; Sato, M.; Ogi, K. JP Patent JP95−18177.7 19950718, 1997.

(38) Chaudhury, N.; Puddephatt, R. J. *J. Organomet. Chem.* **1975**, *84*, 105−115.

(39) Holtcamp, M. W.; Henling, L. M.; Day, M. W.; Labinger, J. A.; Bercaw, J. E. *Inorg. Chim. Acta.* **1998**, *270*, 467−478.

(40) Kostelansky, C. N.; MacDonald, M. G.; White, P. S.; Templeton, J. L. *Organometallics* **2006**, *25*, 2993−2998.

(41) Vedernikov, A. N.; Huffman, J. C.; Caulton, K. G. *New J. Chem.* **2003**, *27*, 665−667.

(42) Vedernikov, A. N.; Caulton, K. G. *Chem. Commun.* **2003**, 358−359.

(43) Albano, V. G.; Castellari, C.; Ferrara, M. L.; Panunzi, A.; Ruffo, F. *J. Organomet. Chem.* **1994**, *469*, 237−244.

(44) De Felice, V.; Ferrara, M. L.; Panunzi, A.; Ruffo, F. *J. Organomet. Chem.* **1992**, *439*, C49−C51.

(45) Johnson, J. A.; Sames, D. *J. Am. Chem. Soc.* **2000**, *122*, 6321−6322.

(46) Johnson, J. A.; Li, N.; Sames, D. *J. Am. Chem. Soc.* **2002**, *124*, 6900−6903.

(47) Wik, B. J.; Lersch, M.; Krivokapic, A.; Tilset, M. *J. Am. Chem. Soc.* **2006**, *128*, 2682−2696.

Table 1. Crystallographic Data and Collection Parameters for **2**

formula	$C_{64}H_{45}BF_{24}N_2Pt{\cdot}C_5H_{12}$
mol wt.	1576.07
crystal system	triclinic
space group	$P\bar{1}$
a, Å	11.9369(5)
b, Å	14.9994(5)
c, Å	18.2760(8)
α, deg	89.172(3)
β, deg	86.881(3)
γ, deg	87.947(3)
V, Å^3	3265.0(2)
Z	2
D_{calc}, mg m^{-3}	1.603
$F(000)$	1568
cryst dimens, mm	0.20 × 0.20 × 0.15
temp, °C	−173
radiation	Mo Kα (0.71073)
theta range, deg	1.12−25.00
μ, mm^{-1}	2.261
reflections collected	20328
R_f	0.0528
R_w	0.0844
GOF	0.972

formed in the presence of excess ethylene. No other oligomeric products such as hexenes or higher olefins were observed. Figure 2 shows a series of ^{1}H NMR spectra which depict the growth of the products over time. 1-Butene can be detected by the appearance of olefinic signals at 5.92, 5.03, and 4.96 ppm and resonances at 2.11 and 1.03 ppm for an ethyl moiety. Resonances for *cis*- and *trans*-2-butene are observed at 1.64 and 1.67 ppm but the olefinic resonances of both *cis*- and *trans*-2-butene are masked by excess ethylene at 5.4 ppm. Isomerization of 1-butene to 2-butene is favored at low ethylene concentrations. Over long times under the reaction conditions, secondary products begin to appear, which likely arise from butenes reacting competitively with ethylene.

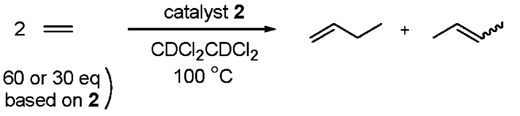

(2)

Kinetic Studies. Migratory Insertion in the Ethylene Hydride Complex 1. Spin-saturation transfer (SST) experiments were carried out to measure the rate of exchange of the hydride with the olefinic hydrogens in **1.** Irradiation and saturation of the ethylene signal in **1** at 64 °C resulted in a substantial decrease in the intensity of the hydride resonance. Combining this data with T_1 data yields an exchange rate of 2.4 s^{-1}, corresponding to a free energy of activation of 19.2 kcal/mol (see Experimental Section for details). Three routes can be envisioned to account for this exchange process (Scheme 3). Route A involves direct formation of the 14-electron intermediate **6** in which all the three hydrogens of the methyl group become equivalent. Routes B and C involve the formation of agostic intermediate **7**. Route B achieves scrambling through an "in-place" rotation of the agostic methyl group (never accessing a true 14-electron species), which has previously been suggested for similar β-agostic ethyl species.[27−30,48−50] Route C accomplishes scrambling from agostic **7** via formation of 14-electron **6**.

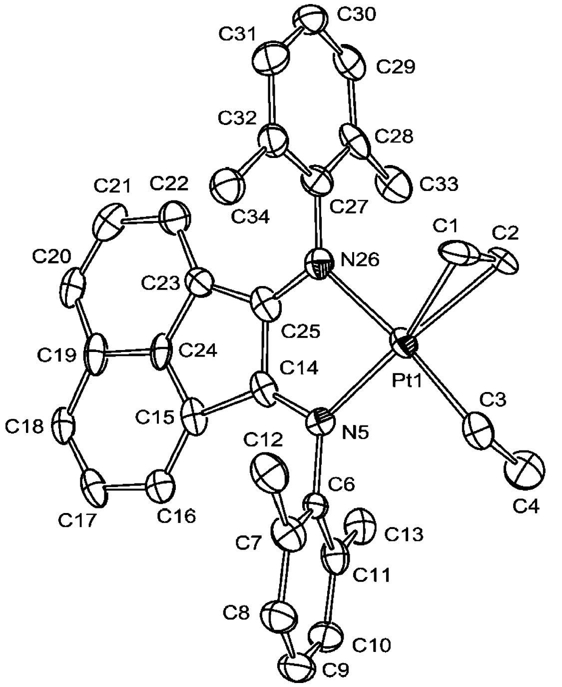

Figure 1. ORTEP drawing of the structure of **2**. Ellipsoids are given with 50% probability. Selected bond distances in angstroms (Å): Pt1−C1 = 2.145(6), Pt1−C2 = 2.151(6), Pt1−C3 = 2.033(7), Pt1−N5 = 2.065(5), Pt1−N26 = 2.181(5), C1−C2 = 1.369(8), C3−C4 = 1.522(9). Selected bond angles in degrees (°): C1−Pt1−C2 = 37.2(2), C1−Pt1−C3 = 90.8(3), C2−Pt1−C3 = 87.9(3), C1−Pt1−N5 = 158.1(2), C1−Pt1−N26 = 96.2(2), C2−Pt1−N5 = 164.3(2), C2−Pt1−N26 = 98.3(2), C3−Pt1−N5 = 93.9(2), C3−Pt1−N26 = 173.0(2), N5−Pt−N26 = 79.26(19).

Kinetics of Ethylene Exchange in 1. We have examined the rate of ethylene self-exchange in complex **1** using ^{1}H NMR line broadening techniques. Exposure of a CD_2Cl_2 solution of **1** at −81 °C to free ethylene results in line broadening of the bound ethylene signal at 4.02 ppm. The change in width at half-height is proportional to ethylene concentration implying that, as expected for a Pt(II) complex, the exchange is associative. The second-order rate constants can be computed using the slow exchange approximation: $k = \pi(\Delta\nu)/[\text{ethylene}]$ ($\Delta\nu$ = change in line width at half-height). Data is summarized in Table 2. The calculated ethylene exchange second-order rate constant using 0.5, 1.0, and 1.5 equiv of ethylene was ca. 1.0×10^5 M$^{-1}\cdot$s^{-1}. This exchange likely proceeds through a five-coordinate species such as **8**.

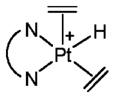

8

Kinetics of Ligand Exchange Reactions in 2 and 5 and Relative Binding Affinities of Ethylene and Acetonitrile. Similar to **1**, bound ethylene in ethyl ethylene complex **2** exhibits associative exchange with free ethylene, and the second-order rate constant can be determined through ^{1}H NMR line-broadening experiments. Experiments were carried out in CD$_2$-

---

(48) Tempel, D. J; Brookhart, M. *Organometallics* **1998**, *17*, 2290−2296.

(49) Shultz, L. H.; Tempel, D. J.; Brookhart, M. *J. Am. Chem. Soc.* **2001**, *123*, 11539−11555.

(50) (a) Derome, A. E.; Green, M. L. H.; Wong, L.-L. *New J. Chem.* **1989**, *13*, 747−753. (b) Bercaw, J. E.; Bugrer, B. J.; Green, M. L. H.; Santarsiero, B. D.; Sella, A.; Trimmer, M.; Wong, L.-L. *J. Chem. Soc., Chem. Commun.* **1989**, *10*, 734−736. (c) McNally, J. P.; Cooper, N. J. *Organometallics* **1988**, *7*, 1704−1715. (d) Casey, C. P.; Yi, C. S. *Organometallics* **1991**, *10*, 33−35.

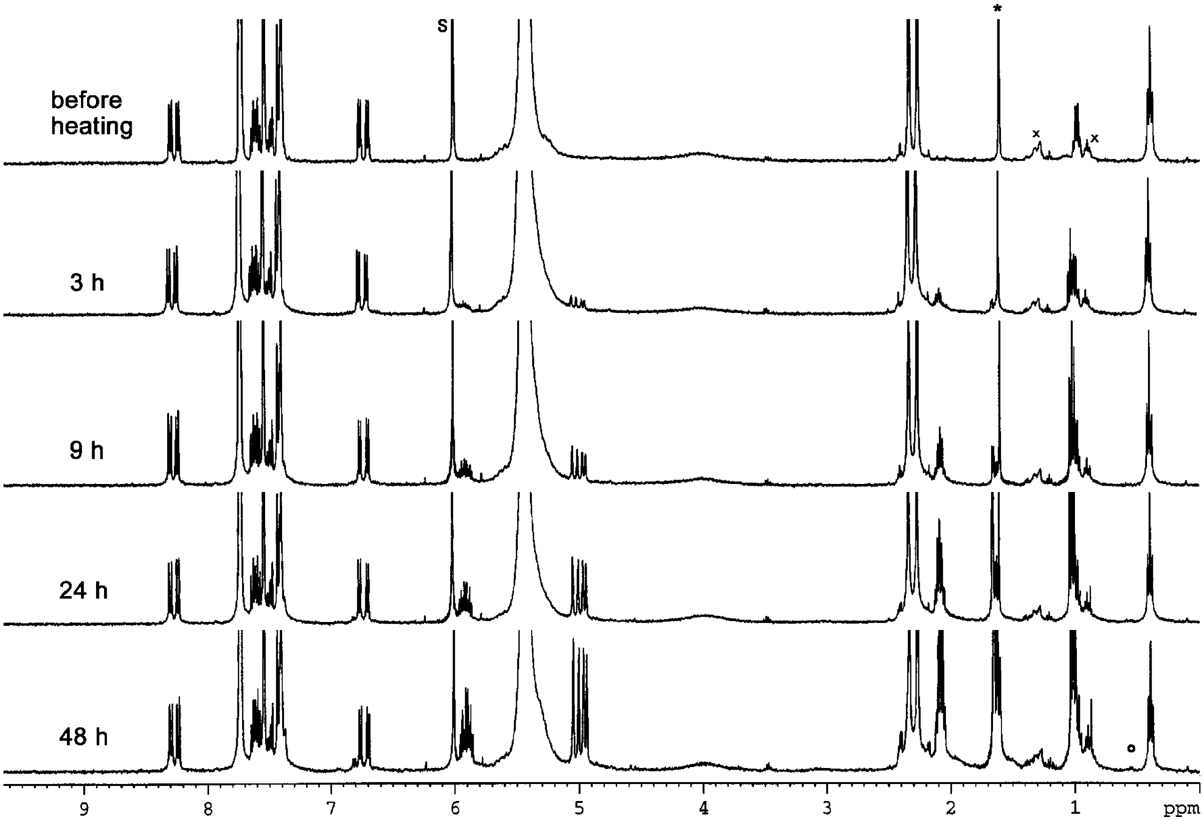

Figure 2. ^{1}H NMR profile depicting growth of 1- and 2-butenes (s: solvent, *: H_2O, ×: impurities, ○: the decomposed Pt complex). The spectra were measured at r.t. Reaction conditions: catalysts **2** (4.5 mM), 60 equiv of ethylene, in $CDCl_2CDCl_2$, heated at 100 °C.

Scheme 3. Possible Pathways for Scrambling Hydride with Hydrogens of Ethylene

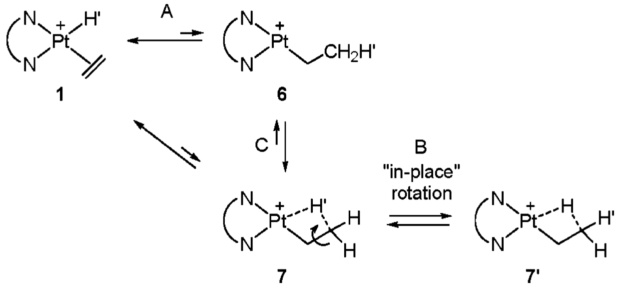

Cl_2 at 27 °C. The change in the line width at half-height of the resonance for the bound ethylene was measured as a function of the concentration of added ethylene, and the second-order rate constants were calculated as above for complex **1**. Kinetic data are summarized in Table 3. The second-order rate of ethylene exchange in **2** is much slower than in **1**. Whereas the second-order exchange rate constant for **2** is ca. 4×10^3 $M^{-1}\cdot s^{-1}$ at 27 °C, even faster exchange rates, ca. 1×10^5 $M^{-1}\cdot s^{-1}$, are observed for **1** at a temperature almost 100 °C lower! The free energies of activation for the two exchange reaction differ by 6 kcal/mol (12.6 vs 6.7 kcal/mol).

Table 2. Kinetic Data from Ethylene Exchanging on **1**[a]

[ethylene] (mM)	half-height line width (Hz)[b]	$\Delta\nu$ (Hz)	k_{obs} (s^{-1})	k ($M^{-1}\cdot s^{-1}$)[c]	$\Delta G^‡$ (kcal/mol)
0.00	9	-	-	-	-
0.63	30	21	6.5×10^1	1.0×10^5	6.7
1.54	62	53	1.7×10^2	1.1×10^5	6.7
2.45	89	80	2.5×10^2	1.0×10^5	6.7

[a] Condition: [**1**] = 3.3 mM, in CD_2Cl_2 at −80.5 °C. [b] Coordinated ethylene peak at 4.02 ppm. [c] k ($M^{-1}\cdot s^{-1}$) = k_{obs}/[ethylene].

Table 3. Kinetic Data from Ethylene Exchanging on **2**[a]

[ethylene] (mM)	half-height width (Hz)[b]	$\Delta\nu$ (Hz)	k_{obs} (s^{-1})	k ($M^{-1}\cdot s^{-1}$)[c]	$\Delta G^‡$ (kcal/mol)
0.0	2.7	-		-	-
3.2	6.5	3.7	1.2×10^1	3.7×10^3	12.6
5.6	9.4	6.7	2.1×10^1	3.7×10^3	12.6
8.3	14.7	12.0	3.8×10^1	4.5×10^3	12.5

[a] Condition: [**2**] = 4.7 mM, in CD_2Cl_2 at 27 °C. [b] Coordinated ethylene peak at 3.96 ppm. [c] k ($M^{-1}\cdot s^{-1}$) = k_{obs}/[ethylene].

In the case of acetonitrile complex **5**, degenerate exchange with free nitrile is sufficiently slow that in the presence of free nitrile no line broadening of the signal for bound nitrile at 2.03 ppm is observed up to temperatures of 24 °C. The rate of ligand exchange was thus monitored by treatment of **5** with excess CD_3CN in CD_2Cl_2 at 24 °C and measuring the decrease in the integral of bound nitrile in **5** and the increase in the signal for free CH_3CN at 1.96 ppm. Second-order kinetics were observed with $k = 6.4 \times 10^{-4}$ $M^{-1}\cdot s^{-1}$, corresponding to $\Delta G^‡ = 21.7$ kcal/mol for a 1.0 M concentration of free ligand (for details of kinetic measurements see Supporting Information).

Prior to measuring the kinetics for interchange of acetonitrile and ethylene in **2** and **5**, the relative binding affinities of the two ligands were determined. Complex **2** (4.5 mM in CD_2Cl_2) was treated with 10 equiv each of CH_3CN and C_2H_4 at 24 °C. The concentrations of **2** and **5** were monitored by ^{1}H NMR spectroscopy. The ratio of **2** : **5** reached a constant value after ca. 1 h and remained constant over the next 3 h. From the ratios of **2** : **5** : ethylene : acetonitrile the equilibrium constant for eq 3 could be estimated as 0.50 corresponding to $\Delta G = +0.4$

Scheme 4. Free Energy Diagrams

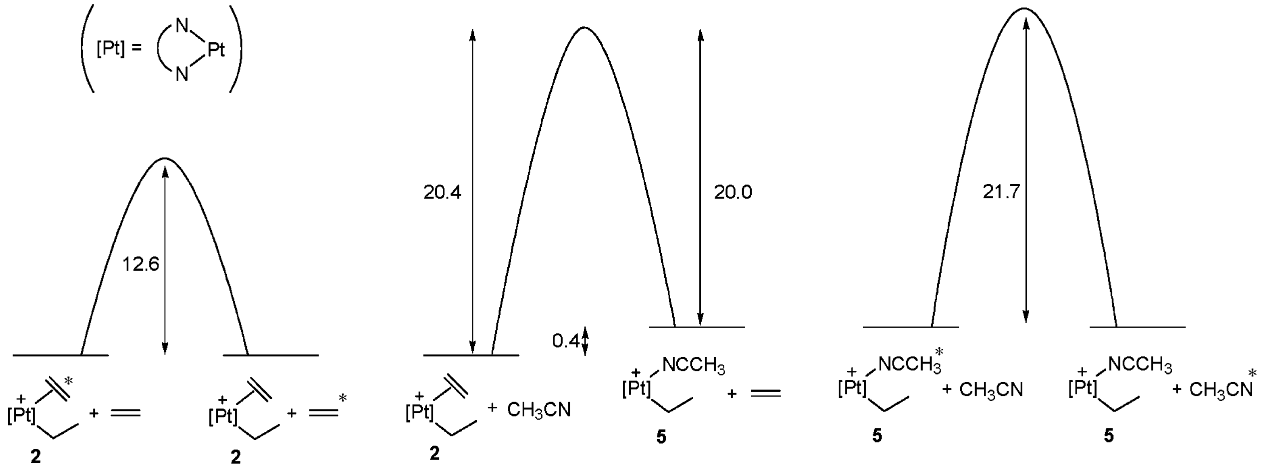

(all values in kcal/mol with second order rate constant normalized to 1 M concentrations)

Table 4. Kinetic Data for the Formation of **2** and **5**[a]

L	equiv of L	k_{obs} (s^{-1})[b]	k ($M^{-1}{\cdot}s^{-1}$)[b]	$\Delta G^\ddagger$ (kcal/mol)
ethylene	10	1.0×10^{-4}	2.2×10^{-3}	15.3
ethylene	30	2.4×10^{-4}	1.8×10^{-3}	15.4
CH_3CN	10	1.4×10^{-4}	3.1×10^{-3}	15.2
CH_3CN	30	4.2×10^{-4}	3.1×10^{-3}	15.2

[a] Condition: [**1**] = 4.5 mM, in CD_2Cl_2 at −54 °C. [b] k_{obs} = pseudo first-order rate constant = k[L].

kcal/mol. Thus the binding affinities of acetonitrile and ethylene in this system are quite similar, with ethylene slightly favored.

The rate of displacement of ethylene from **2** by CH_3CN was

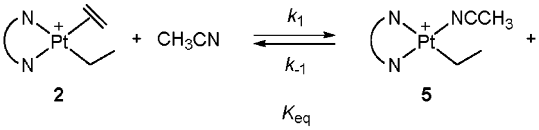

(3)

measured by treatment of **2** with 10 and 30 equiv of CH_3CN in CD_2Cl_2 at 24 °C and monitoring conversion to **5** by ^1H NMR spectroscopy. Second-order kinetics were observed and analyzed, taking into account the final equilibrium ratios of **2**:**5**. The second-order rate constants in eq 3 above were determined to be $k_1 = 5.6 \times 10^{-3}$ $M^{-1}{\cdot}s^{-1}$, $\Delta G^\ddagger = 20.4$ kcal/mol and $k_{-1} = 1.1 \times 10^{-2}$ $M^{-1}{\cdot}s^{-1}$, $\Delta G^\ddagger = 20.0$ kcal/mol.

A summary of the exchange reactions is captured in the free energy diagram in Scheme 4.

Kinetics of Formation of 2 and 5 from 1. Rate constants for the formation of **2** and **5** from **1** were determined by ^1H NMR spectroscopy at −54 °C by adding excess ligand (10 and 30 equiv) to **1** and monitoring formation of **2** and **5**. Kinetics followed pseudo-first order behavior with the formation of both **2** and **5** dependent on the concentration of L. Data are summarized in Table 4. When L is ethylene, the ratio of the two rate constants as a function of ethylene concentration (30:10 equiv) was determined to be 2.4, whereas for acetonitrile, the ratio was 3.0, indicating a first-order dependence on added L in each case.

Are these low-temperature trapping rates compatible with high-temperature scrambling results for a common 14-electron intermediate, **6**? In fact this data is inconsistent with formation of **2** and **5** through trapping of the 14-electron intermediate **6** in Scheme 3. Assuming **6** is responsible for scrambling, extrapolation of the rate of formation of **6** from 65 °C to −54 °C yields a rate constant of 3.0×10^{-7} s^{-1} (assuming a $\Delta S^\ddagger$ of 0 for this intramolecular process), 3 orders of magnitude slower than the observed rate. Although this is a large temperature range for extrapolation, for the extrapolated rate constant to match those in Table 4, a large and positive $\Delta S^\ddagger$ (ca. +30 eu) would need to apply for formation of **6**, and this is clearly unreasonable for an intramolecular migration reaction. Furthermore, because the rate of trapping is dependent on ligand concentration, an additional barrier for trapping must be taken into account, so the rate of formation of **6** predicted from k_1 establishes an upper limit on the rate of trapping (eq 4).

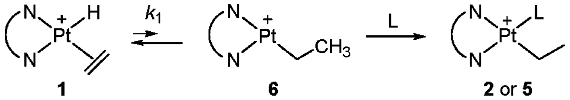

kinetic data inconsistent with this pathway

(4)

After ruling out trapping of **6** as a mechanism of formation of **2** and **5**, two remaining possibilities are summarized in eqs 5 and 6. Equation 5 represents trapping of a reversibly formed agostic intermediate **7**. Because the rate of formation of **2** and **5** depends on [L], k_{-1} must be greater than k_2[L]. Equation 6 represents a distinctly different route to **2** and **5** in which migratory insertion occurs from a five-coordinate intermediate **8**. The kinetic experiments above cannot distinguish between rate-determining formation of **7** or rapid, reversible formation of **8** followed by slow migratory insertion. From ethylene exchange experiments described below, if **8** is involved it is likely formed rapidly and reversibly.

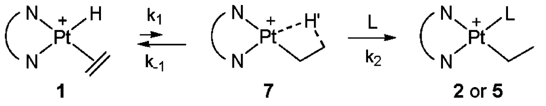

(5)

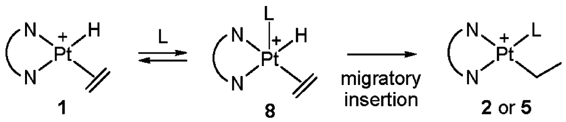

(6)

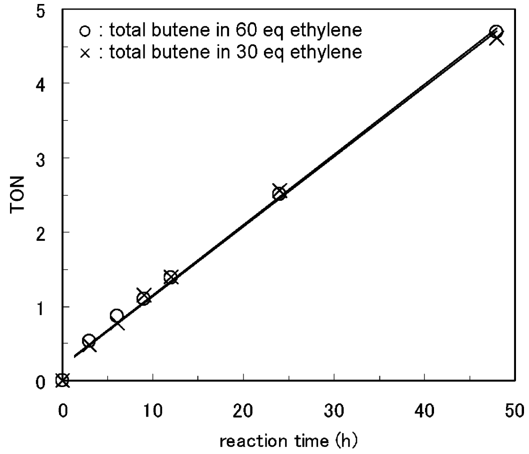

Figure 3. Kinetic Plot for Ethylene Dimerization Catalyzed by **2**.

The structures and dynamics of related complexes bearing bidentate phosphine ligands reported by Spencer, et al. are relevant to the transformation in eq 5.[27−30] Spencer showed that there is a subtle energy balance between the agostic ethyl isomer and the ethylene hydride isomer; the agostic species is favored by both large P−Pt−P bond angles and sterically bulky substituents as shown below for complexes **9**−**11**. Furthermore, judging from the reported temperature-dependent spectra of the β-agostic ethyl species and the related *t*-butyl complex **11** the barrier to "in-place" rotation around the $C_\alpha-C_\beta$ bond in these complexes is substantial, ca. 8−10 kcal/mol.[50]

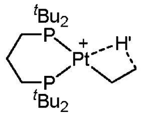

9

β-agostic structure

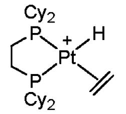

10

ethylene hydride structure

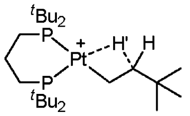

11

β-agostic structure

This data suggests that an agostic intermediate, **7**, should be readily accessible from **1**. If the barrier to in-place rotation in **7** is 8−10 kcal/mol, then the energy barrier between **1** and **7** must be ca. 9−11 kcal/mol to account for the observed exchange barrier of 19.2 kcal/mol. The accessibility of **7** is consistent with a significant barrier to trapping of **7** by ethylene and acetonitrile.

Insertion from a five-coordinate species **8** (eq 6) is appealing based on our previous observations for CO insertion in four- and five-coordinate Ni(II) systems. The insertion barrier in $(dppp)Ni(CO)_2(CH_3)^+$ is 2 kcal/mol lower than insertion in the four-coordinate $(dppe)Ni(CO)(CH_3)^+$.[51] However, the vast difference in rates between degenerate ethylene exchange in **2** and acetonitrile exchange in **5**, both passing through five-coordinate intermediates, makes the five-coordinate insertion pathway less attractive, because ethylene and acetonitrile react with **1** to form **2** and **5**, respectively, at very similar rates. Although kinetically the two pathways cannot be distinguished, we favor the agostic intermediate route shown in eq 5.

Kinetics of Ethylene Dimerization. The ethyl ethylene complex **2** is the catalyst resting state for ethylene dimerization. Analogous complexes are consistent with observations concerning ethylene dimerization and polymerization using Pd and Ni diimine analogues.[12,14−18] The turnover-limiting step is the migratory insertion of ethylene into the Pt−Et bond to form a Pt-*n*-butyl intermediate. The turnover frequency (TOF) of ethylene dimerization catalyzed by **2** was determined by ^{1}H NMR spectroscopy. The reaction was carried out in $CDCl_2$-$CDCl_2$ at 100 °C using two different concentrations of ethylene, 30 and 60 equiv relative to the platinum catalyst. Figure 3 shows a plot of reaction time versus turnover number (TON) calculated from the total amount of 1- and *cis*- and *trans*-2-butenes formed (one turnover consumes two equivalents of ethylene). The results clearly show that the dimerization rate is independent of ethylene concentration. From qualitative observations it appears that the rate of isomerization of 1-butene to 2-butenes decreases as ethylene concentration increases. After 48 h at 100 °C, the product ratios were 1-butene:*cis*-2-butene:*trans*-2-butene = 28:21:51 for the experiment with 30 equiv ethylene and 55:13:32 with 60 equiv ethylene. The rate constant for migratory insertion of **2** calculated from the TOF is 2.61×10^{-5} s^{-1} corresponding to $\Delta G^\ddagger = 29.8$ kcal/mol. Kinetic data are summarized in Table 5.

Table 5. Kinetic Data for Ethylene Dimerization Catalyzed by **2**[a]

equiv of ethylene	k (s^{-1})	$\Delta G^\ddagger$ (kcal/mol)
30	2.60×10^{-5}	29.8
60	2.62×10^{-5}	29.8

[a] Condition: [**2**] = 4.5 mM, in CD_2ClCD_2Cl at 100 °C.

Scheme 5. Isomerization of the 1-Butene Complex **3**

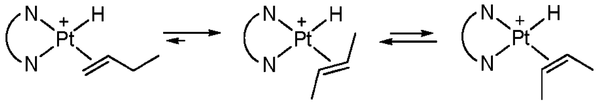

3 *trans*-**12** *cis*-**12**

(**3**:*trans*-**12**:*cis*-**12** = 1:10:7)

Synthesis and Reactivity of [(N^N)Pt(H)(1-butene)][BAr′$_4$] (3). The (N^N)Pt(H)(η^2-1-butene)$^+$ complex (**3**) is presumed to be an intermediate in the catalytic ethylene dimerization by **2**. This complex could be isolated via displacement of ethylene from **1** with 1-butene. Addition of a large excess of 1-butene to a solution of **1** in CH_2Cl_2 at −78 °C followed by vacuum removal of volatiles produced pure complex **3** as an orange powder (eq 7). (If the reaction solution is warmed during the ligand exchange a complex mixture of products is obtained.) Complex **3** is reasonably stable in the solid state, remaining unchanged at room temperature for at least one week. In solution above 0 °C, **3** readily isomerizes to yield mixtures of **3** and the *cis*- and *trans*-2-butene complexes, *cis*- and *trans*-**12**. The equilibrium ratios are specified in Scheme 5. Spectroscopic characterization of **3** and the isomeric 2-butene complexes **12** are described in the Experimental Section.

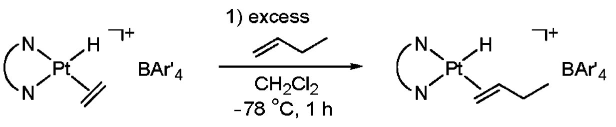

1 **3** (80%) (7)

The reaction of complex **3** with ethylene was examined at low temperatures. Upon addition of 2 equiv of ethylene to a CD_2Cl_2 solution of **3** at −78 °C, the ethylene hydride complex **3** and free 1-butene were observed by ^{1}H NMR spectroscopy at −78 °C (eq 8). The reaction proceeds extremely rapidly at

---

(51) Shultz, C. S.; DeSimone, J. M.; Brookhart, M. *J. Am. Chem. Soc.* **2001**, *123*, 9172−9173.

Scheme 6. Catalytic Cycle of Ethylene Dimerization Catalyzed by **2**

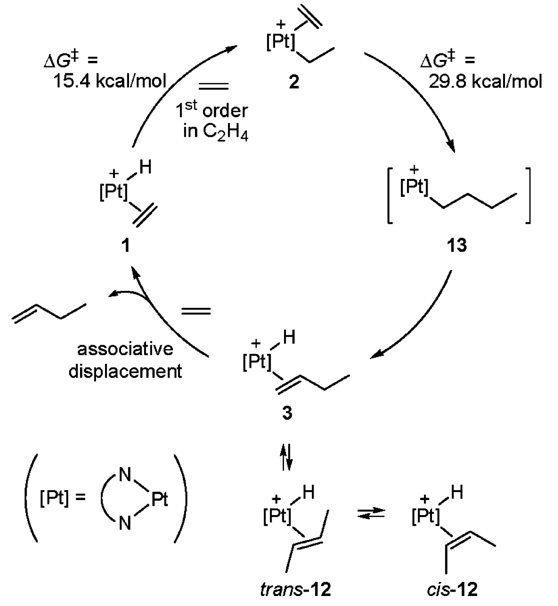

-78 °C as expected from the observation of very rapid degenerate ethylene exchange in **1**. Kinetics cannot be measured, but it seems safe to assume this is an associative displacement.

Catalytic Cycle for Ethylene Dimerization. A complete catalytic cycle for ethylene dimerization can now be proposed (Scheme 6). Three intermediates (**1**, **2**, and **3)** have been isolated and fully characterized. Complex **2** is the catalyst resting state and undergoes first-order migratory insertion ($\Delta G^{\ddagger} = 29.8$ kcal/mol) to form the butyl complex **13** which, following β-hydrogen elimination, produces the 1-butene hydride, **3**. Ethylene very rapidly displaces 1-butene from **3** to yield ethylene hydride **1**. Alternatively **3** can isomerize to *cis*-**12** and *trans*-**12** which, upon reaction with ethylene, yields *cis*- and *trans*-2-butenes and **1**. Higher ethylene concentrations result in more rapid interception of **3** and higher fractions of 1-butene product. To close the catalytic cycle, ethylene hydride **1** converts to **2** via a process which is first-order in ethylene ($\Delta G^{\ddagger} = 15.4$ kcal/mol).

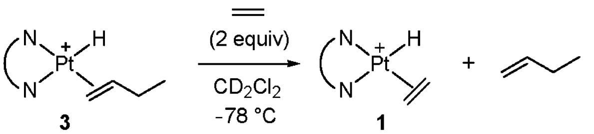

(8)

Concluding Remarks

Three key intermediates in this Pt-based catalytic system for dimerization of ethylene have been isolated and characterized: ethylene hydride complex **1**, ethyl ethylene complex **2**, and butene hydride **3**. Kinetic studies have provided detailed information concerning the nature and the energetics of each step. Perhaps most instructive is the observation that the conversion of ethylene hydride **1** to ethyl ethylene complex **2** is first-order in ethylene and *does not* involve trapping of a true fourteen-electron (diimine)$PtCH_2CH_3^+$ intermediate. We cannot distinguish between pathways involving either ethylene trapping of a reversibly formed β-agostic ethyl intermediate or migratory insertion of a reversibly formed five-coordinate bis-ethylene hydride. Conversion of ethyl ethylene complex **2** to the Pt-butyl species is not assisted by ethylene and appears to be a simple first-order migratory insertion reaction. It is informative to compare this barrier, 29.6 kcal/mol, to barriers measured for analogous (diimine)Ni(R)(ethylene)$^+$ species (13−14 kcal/mol) and (diimine)Pd(R)(ethylene)$^+$ species (17−19 kcal/mol).[12,14−18] DFT computations on related species are in general agreement with these trends and the observation that there is a much greater difference in the migration barriers between the second and third row systems than between the first and second row systems.[21−23] DFT calculations also are consistent with the observation that the Pt ethylene hydride is a classical hydride whereas the Ni and Pd systems exist as β-agostic alkyl complexes.

Experimental Section

General Methods. All manipulations were performed using standard Schlenk techniques. Nitrogen was purified by passage through columns of BASF R3−11 catalyst (Chemalog) and 4 Å molecular sieves. ^1H and ^{13}C NMR spectra were recorded on a Bruker Avance 400 MHz. Chemical shifts are reported relative to solvent peaks (CD_2Cl_2: δ 5.32 for ^1H, δ 53.8 for ^{13}C, $CDCl_2CDCl_2$: δ 6.02 for ^1H). Elemental analyses were performed by Atlantic Microlab of Norcross, GA. Probe temperatures in NMR experiments were measured using the MeOH calibration method.

Materials. Methylene chloride, toluene, diethyl ether, acetonitrile, and pentane were purified using procedures reported by Pangborn et al.[52] Methylene chloride-d_2 and 1,1,2,2-tetrachloroethane-d_2 were purchased from Cambridge Isotope Laboratories. Methylene chloride-d_2 was dried over CaH_2 and then distilled by vacuum transfer, whereas 1,1,2,2-tetrachloroethane-d_2 was used without further purification. Polymer-grade ethylene and 1-butene were purchased from Matheson Tri-Gas and Aldrich, respectively, and used without further purification. The α-diimine ligand (N^N),[53−55] (cod)$PtEt_2$,[56] and $[H(OEt_2)_2][BAr'_4]$[57] were prepared based on standard literature procedures.

Representative $BAr'_4{}^-$ NMR Data. ^1H and ^{13}C data for the $BAr'_4{}^-$ counterion are reported separately for simplicity. ^1H NMR (CD_2Cl_2): δ 7.77 (br, 8H, *o*-Ar′), 7.60 (br, 4H, *p*-Ar′). ^{13}C NMR (CD_2Cl_2): δ 162.1 (1:1:1:1 pattern, $^1J_{B-C} = 51$ Hz, C_{ipso}), 135.3 (C_{ortho}), 129.4 (qq, $^2J_{C-F} = 30$ Hz, $^4J_{C-F} = 5$ Hz, C_{meta}), 125.0 (q, $^1J_{C-F} = 295$ Hz, CF_3), 117.8 (C_{para}).

$[(2,6\text{-}Me_2C_6H_3)N{=}C(An){-}C(An){=}N(2,6\text{-}Me_2C_6H_3)]PtEt_2$ (4). A solution of α-diimine ligand (N^N) (772 mg, 1.99 mmol) in acetonitrile (50 mL) was added to a solution of (cod)$PtEt_2$ (598 mg, 1.65 mmol) in acetonitrile (10 mL) at room temperature. The dark orange solution was stirred at 55 °C for 16 h. After cooling, all solvents were removed on a vacuum line leaving a green solid. The residue was dissolved in toluene and purified by column chromatography (alumina, toluene). From the collected green solution, toluene was removed under vacuum. Recrystallization from CH_2Cl_2/pentane, filtration, and drying in vacuo gave 668 mg (63% yield) of **4** as green microcrystals. ^1H NMR (CD_2Cl_2, 400 MHz): δ 8.28 (d, 2H, $J = 8.4$ Hz, An-*p*H), 7.33 (m, 8H, An-*m*H, ArH), 6.81 (d, 2H, $J = 7.2$ Hz, An-*o*H), 2.30 (s, 12H, $ArCH_3$), 2.05 (q, 2H, $^3J_{H-H} = 7.6$ Hz, $^2J_{Pt}{-}H = 94.8$ Hz, $PtCH_2CH_3$), 0.73 (t, 3H, $^3J_{H-H} = 7.6$ Hz, $^3J_{Pt-H} = 85.2$ Hz, $PtCH_2CH_3$). ^{13}C NMR (CD_2Cl_2, 400 MHz): δ 170.0, 146.0, 143.4, 133.2, 130.9, 130.4, 129.4, 128.6 (overlapped), 126.7, 121.1 ($J_{Pt-C} = 59$ Hz), 17.8 ($PtCH_2CH_3$), 17.5 ($ArCH_3$), −0.3 ($PtCH_2CH_3$, $^1J_{Pt-C} = 886$ Hz). Anal. Calcd for $C_{32}H_{34}N_2Pt$: C, 59.89; H, 5.34; N, 4.37. Found: C, 59.87; H, 5.47; N, 4.44.

---

(52) Pangborn, A. B.; Giardello, M. A.; Grubbs, R. H.; Rosen, R. K.; Timmers, F. J. *Organometallics* **1996**, *15*, 1518−1520.
(53) van Asselt, R.; Elsevier, C. J.; Smeets, W. J. J.; Spek, A. L.; Benedix, R. *Recl. Trav. Chim. Pays-Bas* **1994**, *113*, 88−98.
(54) tom Dieck, H.; Svoboda, M.; Grieser, T. *Naturforsch* **1981**, *36b*, 823−832.
(55) Svoboda, M.; tom Dieck, H. *J. Organomet. Chem.* **1980**, *191*, 321−328.
(56) Clark, H. C.; Manzer, L. E. *J. Organomet. Chem.* **1973**, *59*, 411−428.
(57) Brookhart, M.; Grant, B.; Volpe, A. F. *Organometallics* **1992**, *11*, 3920−3922.

[[(2,6-$Me_2C_6H_3$)N═C(An)−C(An)═N(2,6-$Me_2C_6H_3$)]Pt(H)(ethylene)][BAr′$_4$] (1). A solution of [H(OEt_2)$_2$][BAr′$_4$] (127 mg, 0.126 mmol) in diethyl ether (10 mL) cooled to −78 °C was added dropwise to a solution of diethyl complex **4** (80.2 mg, 0.125 mmol) in diethyl ether (40 mL) at −78 °C via a cannula. The combined solutions were placed under vacuum at −78 °C for 4.5 h then warmed to r.t. where solvents were removed under vacuum. Recrystallization of the orange residue from CH_2Cl_2/pentane and filtration was repeated until the supernatant had no purple color. Drying under vacuum gave 149.4 mg of **1** as light orange powder (81% yield). ^{1}H NMR (CD_2Cl_2, 400 MHz): δ 8.28 (d, 1H, *J* = 8.4 Hz, An-*p*H), 8.25 (d, 1H, *J* = 8.4 Hz, An-*p*H), 7.61−7.57 (m, 2H, An-*o*H), 7.40−7.37 (m, 6H, ArH), 6.84 (d, 1H, *J* = 8.8 Hz, An-*o*H), 6.82 (d, 1H, *J* = 8.8 Hz, An-*o*H), 4.02 (brs, 4H,$^2J_{Pt-H}$ = 64.4 Hz, CH_2═CH_2), 2.42 (s, 6H, ArC*H*$_3$), 2.31 (s, 6H, ArC*H*$_3$), −21.7 (s, 1H,$^1J_{Pt-H}$ = 1107 Hz, Pt−H). ^{13}C NMR (CD_2Cl_2, 400 MHz): δ 178.0, 175.1, 149.1, 146.4, 142.0, 134.6, 133.8, 132.1, 130.6, 130.5, 130.1, 130.0, 129.5, 129.4, 128.8, 128.2, 126.5, 125.9, 124.5, 124.4, 69.9 (CH_2═CH_2), 18.2 (Ar*C*H$_3$), 17.8 (Ar*C*H$_3$), Anal. Calcd for $C_{62}H_{41}BF_{24}N_2Pt$: C, 50.46; H, 2.80; N, 1.90. Found: C, 50.78; H, 2.78; N, 1.88.

[[(2,6-$Me_2C_6H_3$)N═C(An)−C(An)═N(2,6-$Me_2C_6H_3$)]Pt(Et)(ethylene)][BAr′$_4$] (2). A solution of complex **1** (100 mg, 67.8 mmol) in CH_2Cl_2 (3.0 mL) at 0 °C was purged with ethylene for 5 min. Pentane (20 mL) was then added to form an orange precipitate which was collected by filtration and dried under vacuum to give 89.6 mg (88% yield) of the isolated product **2**. ^{1}H NMR (CD_2Cl_2, 400 MHz): δ 8.31 (d, 1H, *J* = 8.3 Hz, An-*p*H), 8.25 (d, 1H, *J* = 8.5 Hz, An-*p*H), 7.63−7.39 (m, 8H, An-*m*H, ArH), 6.81 (d, 1H, *J* = 7.2 Hz, An-*o*H), 6.74 (d, 1H, *J* = 7.5 Hz, An-*o*H), 3.96 (brs, 4H,$^2J_{Pt-H}$ = 71.5 Hz, CH_2═CH_2), 2.37 (s, 6H, ArC*H*$_3$), 2.28 (s, 6H, ArC*H*$_3$), 0.99 (q, 2H,$^3J_{H-H}$ = 7.6 Hz, $^2J_{Pt-H}$ = 74.0 Hz, PtC*H*$_2$CH$_3$), 0.39 (t, 3H,$^3J_{H-H}$ = 7.6 Hz, PtCH$_2$C*H*$_3$). ^{13}C NMR (CD_2Cl_2, 400 MHz): δ 179.8, 172.1, 148.4, 140.8, 140.2, 133.3, 132.1, 130.5, 130.4, 130.1, 130.1 (overlapped), 130.0, 129.8, 129.3, 128.2, 127.3, 125.6, 125.5, 124.7, 75.5 ($^1J_{Pt-H}$ = 212.6 Hz, CH_2═CH_2), 18.1 (Ar*C*H$_3$), 17.5 (Ar*C*H$_3$), 13.5 (PtCH$_2$*C*H$_3$,$^2J_{Pt-H}$ = 146.9 Hz), 9.7 (Pt*C*H$_2$CH$_3$,$^1J_{Pt-H}$ = 637.4 Hz). Anal. Calcd for $C_{64}H_{45}BF_{24}N_2Pt$: C, 51.11; H, 3.02; N, 1.86. Found: C, 51.12; H, 2.94; N, 1.85.

[[(2,6-$Me_2C_6H_3$)N═C(An)−C(An)═N(2,6-$Me_2C_6H_3$)]Pt(Et)(CH_3CN)][BAr′$_4$] (5). To a solution of complex **1** (49 mg) in CH_2Cl_2 (10 mL) was added CH_3CN (1 mL) at −78 °C, and then warmed up to r.t. After 30 min, solvent and excess CH_3CN were evaporated by vacuum to give deep orange residue. The formation of **5** was confirmed by ^{1}H and ^{13}C NMR spectra. ^{1}H NMR (CD_2Cl_2, 400 MHz): δ 8.27 (d, 1H, *J* = 11.2 Hz, An-*p*H), 8.22 (d, 1H, *J* = 11.2 Hz, An-*p*H), 7.56−7.29 (m, 8H, An-*m*H, ArH), 6.81 (d, 1H, *J* = 7.2 Hz, An-*o*H), 6.74 (d, 1H, *J* = 7.3 Hz, An-*o*H), 2.37 (s, 6H, ArC*H*$_3$), 2.27 (s, 6H, ArC*H*$_3$), 2.03 (brs, 3H, NCC*H*$_3$), 1.54 (q, 2H,$^3J_{H-H}$ = 7.6 Hz,$^2J_{Pt-H}$ = 85.9 Hz, PtCH$_2$), 0.58 (t, 3H,$^3J_{H-H}$ = 7.6 Hz,$^3J_{Pt-H}$ = 38.2 Hz, PtCH$_2$C*H*$_3$). ^{13}C NMR (CD_2Cl_2, 100 MHz): δ 178.5, 170.6, 147.3, 142.5, 141.8, 133.1, 132.3, 132.2, 130.5, 130.3 (overlapped), 129.8, 129.5, 129.3, 128.9, 128.5, 126.2, 125.8, 125.1, 124.4, 118.3 (CH$_3$*C*N), 17.8 (ArCH$_3$), 17.5 (ArCH$_3$), 16.7 (*C*H$_3$CN), 4.1 ($^1J_{Pt-C}$ = 445.3 Hz, PtCH$_2$), 3.0 (PtCH$_2$*C*H$_3$).

[[(2,6-$Me_2C_6H_3$)N═C(An)−C(An)═N(2,6-$Me_2C_6H_3$)]Pt(H)(1-butene)][BAr′$_4$] (3). An excess amount of 1-butene (∼1 mL as a liquid at −78 °C) was added to a solution of complex **1** (50 mg, 36 *μ*mol) in CH_2Cl_2 (21 mL) at −78 °C. After stirring at −78 °C for 1 h, methylene chloride and excess 1-butene were evaporated under vacuum while keeping the solution temperature under 0 °C. Complete solvent removal gave **3** in 80% isolated yield as an orange powder. ^{1}H NMR (CD_2Cl_2, 400 MHz, 0 °C): δ 8.28 (d, 1H, *J* = 8.3 Hz, An-*p*H), 8.24 (d, 1H, *J* = 8.4 Hz, An-*p*H), 7.61−7.56 (m, 2H, An-*m*H), 7.40−7.36 (m, 6H, ArH), 6.81 (d, 1H, *J* = 7.4 Hz, An-*o*H), 6.78 (d, 1H, *J* = 7.3 Hz, An-*o*H), 4.62 (m, 1H,$^2J_{Pt-H}$ = 73.8 Hz, vinyl H), 3.98 (d, *J* = 14.0 Hz,$^2J_{Pt-H}$ = 57.8 Hz, vinyl H), 3.83 (d, *J* = 7.8 Hz,$^2J_{Pt-H}$ = 63.7 Hz, vinyl H), 2.42 (s, 3H, ArMe), 2.41 (s, 3H, ArMe), 2.34 (s, 3H, ArMe), 2.27 (s, 3H, ArMe), 2.12−1.98 (m, 2H, CH$_2$ of 1-butene), 1.14 (t, 3H, *J* = 7.2 Hz, CH$_3$ of 1-butene), −23.6 (s, 1H,$^1J_{Pt-H}$ = 1267.7 Hz, Pt−H). ^{13}C NMR (CD_2Cl_2, 100 MHz, at 0 °C): δ 178.1, 174.2, 148.7, 145.7, 141.0, 134.4, 133.4, 131.7, 131.2, 130.6, 130.5, 130.1, 130.1, 130.0, 130.0, 129.3, 128.7, 128.5, 128.0 (overlapped), 126.4, 125.6, 124.2, 123.9, 101.9 (internal *sp*^{2}-C of 1-butene), 68.0 (terminal *sp*^{2}-C of 1-butene), 30.9 (CH$_2$ of 1-butene), 18.1 (Ar*C*H$_3$), 18.1 (Ar*C*H$_3$), 17.7 (Ar*C*H$_3$), 17.5 (Ar*C*H$_3$), 14.1 (Me of 1-butene). Anal. Calcd for $C_{64}H_{45}BF_{24}N_2Pt$: C, 51.11; H, 3.02; N, 1.86. Found: C, 51.37; H, 3.15; N, 1.88.

[[(2,6-$Me_2C_6H_3$)N═C(An)−C(An)═N(2,6-$Me_2C_6H_3$)]Pt(H)(*cis*- and *trans*-2-butene)][BAr′$_4$] (*cis*- and *trans*-12). These isomers were generated by warming **3** in CD_2Cl_2 solution at r.t. to establish an equilibrium between **3** and *cis*- and *trans*-**12**. ^{1}H NMR(CD_2Cl_2, 400Mhz): *trans*-**12:** The aromatic signals of the α-diimine ligand (N^N) overlap the signals of the other isomers. δ 4.49 (q, 2H, *J* = 4.0 Hz,$^2J_{Pt-H}$ = ca. 77 Hz vinyl H), 2.49 (s, 3H, ArMe), 2.42 (s, 3H, ArMe), 2.40 (s, 3H, ArMe), 2.20 (s, 3H, ArMe), 1.76 (d, 6H, *J* = 4.8 Hz,$^3J_{Pt-H}$ = 45.2 Hz, CH$_3$ of *trans*-2-butene), −24.1 (s, 1H,$^1J_{Pt-H}$ = 1317.7 Hz, Pt−H). *cis*-**12**: The aromatic signals of the α-diimine ligand (N^N) overlap the signals of the other isomers. δ 4.47 (m, 2H,$^2J_{Pt-H}$ = ca. 81 Hz, vinyl H), 2.43 (s, 6H, ArMe), 2.33 (s, 6H, ArMe), 2.01 (d, 6H, *J* = 4.4 Hz,$^3J_{Pt}$−H = 63.2 Hz, CH$_3$ of *cis*-2-butene), −24.5 (s, 1H,$^1J_{Pt-H}$ = 1419.3 Hz, Pt−H).

Ethylene Dimerization. For the kinetic study of ethylene dimerization catalyzed by **2**, the sample was prepared as follows: The catalyst **2** (4.0 mg, 2.7 *μ*mol) was added to a tared J-Young tube(Wilmad). After adding $CDCl_2CDCl_2$ (0.60 mL), the tube was capped with a J-Young valve equipped with a rubber capped terminated glass tube. The solution was subjected to three freeze−pump−thaw cycles. Then ethylene gas (2.0−4.0 mL gas at 25 °C, 30−60 equiv based on **2**) was injected via gastight syringe through the rubber cap into the frozen solution (liquid N_2). The J-Young valve was closed and the tube was warmed to room temperature. The ethylene dimerization was carried out by immersing the tube in a 100 °C oil bath. The reaction was quenched at various time intervals in a stream of air (25 °C). Turnover numbers at these intervals were determined by ^{1}H NMR spectroscopy at room-temperature based on the integrals of all three butene isomers: one of the vinyl protons of 1-butene (4.96 ppm) and methyl groups of *cis*- and *trans*-2-butenes (1.64 and 1.66 ppm, respectively). Plots of TON versus time are shown in Figure 3.

Rates of Formation of 2 and 5 from 1. The rates were determined by ^{1}H NMR measurements on samples prepared by the following method: Complex **1** (4.0 mg, 2.7 *μ*mol) was weighed into a tared NMR tube and then dissolved in CD_2Cl_2 (0.60 mL). After cooling the solution to −78 °C, the ligand (either ethylene for **2** or acetonitrile for **5**) was added via gastight syringe or a microsyringe. The tube was then transferred into a −78 °C precooled NMR probe. The reaction was started by warming to −54.2 °C for both **2** and **5**. The hydride signal of starting complex **1** at −21.7 ppm was used to calculate the amount of the remaining **1**. Kinetic plots are shown in Figure S1 (see Supporting Information).

Spin Saturation Transfer Measurement of the Rate of Exchange of the Pt Hydride with the Vinyl Hydrogens of Ethylene. Complex **1** (8.0 mg) in an NMR tube was dissolved in $CDCl_2CDCl_2$ and degassed via three freeze−pump−thaw cycles. At 64.4 °C, the coordinated ethylene signal (4.06 ppm) of **1** was saturated by irradiation, and the decrease in intensity of the hydride (−21.7 ppm) was measured. The relaxation time T_1 for the hydride was determined to be 1.000 s using the inversion−recovery method and analyzed with the spectrometer T_1 routine. The exchange rate constant was calculated using the equation $k_{obs} = (1/T_1)(M(0)/M(\text{irr})-1) = 1.62\ s^{-1}$ where $M(0)$ and M(irr) are the intensities of the hydride resonance before and after spin saturation, respectively. The rate constant *k* for migration was calculated using the equation $k = (3/2)k_{obs} = 2.43\ s^{-1}$ assuming that for every three migration events only two hydrogens undergo site exchange.

Degenerate Ethylene Exchange Rates in 1 and 2. The exchange rate between free ethylene and the coordinated ethylene of **1** and **2** was determined by ^1H NMR line broadening experiments at 192.5 and 298 K, respectively. Samples were prepared by following procedure: In an argon-filled drybox, the corresponding complex was weighed (4 mg) into a tared NMR tube and then dissolved in dry, degassed CD_2Cl_2 (0.60 mL) at room temperature to give a homogeneous solution. After capping with a septum and Parafilm, the NMR spectrum was acquired at the appropriate temperature for each complex. Ethylene gas was added to the solution via a gastight syringe and a second NMR spectrum acquired at the corresponding temperature. The molarities of free ethylene and the ethylene complex were calculated using the BAr'_4 resonances as an internal standard. Linewidths (w) were measured at half-height in units of Hertz for complexed ethylene. Linewidths (w_0) in the absence of ethylene were also measured. The second-order exchange rates were determined from the standard equation for the slow exchange approximation: $k = \pi(\Delta\nu)/[\text{ethylene}]$, where $\Delta\nu$ is equal to $w - w_0$ and [ethylene] is the molar concentration of free ethylene. Data are summarized in Tables 2 and 3.

X-ray Structure of $[[(2,6\text{-}Me_2C_6H_3)N{=}C(An){-}C(An){=}N(2,6\text{-}Me_2C_6H_3)]Pt(Et)(ethylene)][BAr'_4]$ (2). Crystals of **2** were grown from slow diffusion of pentane into a CH_2Cl_2 solution of **2**. The X-ray data were collected on a Bruker SMART APEX-II using the ω scan mode. Experimental details are given in Table 1. The structure was solved by direct methods using SHELXS-97. Final agreement indices were $R_f = 5.3\%$ and $R_w = 8.4\%$, with hydrogen placed in computed positions and included in the refinement using a riding model. All other atoms were refined anisotropically.

Acknowledgment. We thank the National Science Foundation (CHE-0414726(JLT) and CHE-0615704(MB)) for support of this work.

Supporting Information Available: Kinetic plots for rates of formation of **2** and **5** from **1**, the rate of formation of **5** from **2**, the rate of degenerate acetonitrile exchange in **5**, and a plot showing the determination of the equilibration of **2** and **5.** CIF file for complex **2**. This material is available free of charge via the Internet at http://pubs.acs.org.

JA068118O